The use of integral transformations in the study of the propagation of laser beams in dielectrics materials

Leonardo de Sousa Rodrigues

June, 2020

Professor Stefano de Leo

Abstract

Using gaussian type distributions, it is intended to find analytical forms for the behavior of optical beams that propagate in dielectric materials and study lateral displacements. The analytical calculations will be tested using numerical simulations in *Mathematica* to determine if the approximations are reasonable and the regions where they misbehave.

Contents

1 Introduction

Since laser discovery, many uses have progressively shown up in many areas. Nowadays, lasers applications are as diverse as they can be, spread all over medicine, industry, commerce and, evidently, science. Very often, it is necessary to know the behavior of a beam.

The propagation characteristics of lasers depend on its type. However, a considerable part of them behave like a Gaussian beam, i.e., their electric and magnetic fields are Gaussian distributions, as is the light intensity. Furthermore, non Gaussian beams can usually be approximated to a Gaussian one and, when refracted by lens, a Gaussian beam is transformed into another Gaussian beam, which explains why Gaussian optics is a convenient, widespread model in laser optics and its study of great value.

In the first part of this study, the formalism to describe the behavior of a Gaussian beam is developed. Some approximations are used to allow the integrals to be solved analytically. Then, the results are compared to numerical values obtained on simulations using *Mathematica* to ensure the approximations are reasonable.

After that, the refraction of laser beams is analyzed, making possible the determination of its path through a dielectric prism in cases of partial internal reflection - on which Snell's law and some geometry provide the correct lateral displacement - and total internal reflection - where the additional Goos-Hänchen shift is observed.

2 Free Gaussian beams

To analyze the behavior of a beam going through a media change, it is necessary to understand how it propagates and how its electric field can lead to the light intensity distribution in space. As figure 1 shows, the beams studied here have a Gaussian intensity profile. That implies that their wave phase must be convoluted with a Gaussian distribution to get the electric field. [1]

As a Gaussian distribution doesn't have a delimited end, the radius of the beam must be defined in some way. A common method, which will be used here, is to define the radius of the beam as the distance from the center to the point on which the intensity is $1/e^2$ of its maximum value. We'll denote the radius of the beam by $\mathrm{w}(z)$.

A Gaussian beam is defined by its smaller radius w_0 and by the laser wavelength λ. For each point in space, a wave vector $\boldsymbol{k}$ can be assigned, with $k = 2\pi/\lambda$. Note that it is not perfectly uniform as the wavefront has a small curvature. The laser frequency ω can be approximated to constant so that it is not necessary to consider the time dependence $e^{-i\omega t}$. [1]

As said before, the flat wave, $e^{i\boldsymbol{k}\cdot\boldsymbol{r}}$, must be convoluted with a Gaussian distribution, as shown in (2.1). This equation will first be solved analytically and then used for the numeric simulations.

$$E(x,y,z) = E_0 \frac{\mathrm{w}_0^2}{4\pi} \int_{-\infty}^{+\infty} dk_x \int_{-\infty}^{+\infty} dk_y \exp\left[-\frac{\mathrm{w}_0^2}{4}(k_x^2 + k_y^2)\right] \exp\left[i(k_x x + k_y y + k_z z)\right] \tag{2.1}$$

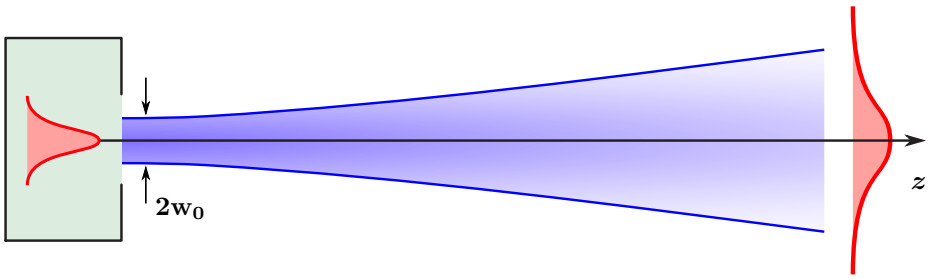

Figure 1: Side view of a Gaussian beam and its source. Note the Gaussian intensity profile and how it spreads as z increases.

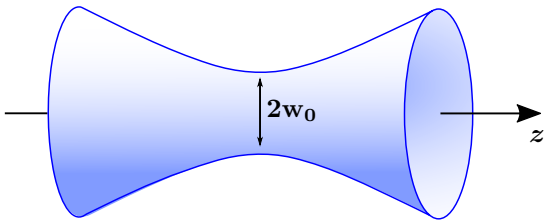

Figure 2: Free laser beam propagating on z axis.

2.1 Analytical development

In this section, (2.1) will be solved analytically. Note that

$$\boldsymbol{k} = (k_x, k_y, k_z) \rightarrow k = \sqrt{k_x^2 + k_y^2 + k_z^2} \rightarrow k_z = k\sqrt{1 - \frac{k_x^2 + k_y^2}{k^2}}$$

Using series form to first order,

$$k_z \approx k - \frac{k_x^2 + k_y^2}{2k} \tag{2.2}$$

Replacing (2.2) in (2.1), the integral can be broken, getting to

$$E(x, y, z) = E_0 \times e^{ikz} \times D_x \times D_y \tag{2.3}$$

Where

$$D_x = \frac{\mathrm{w}_0}{2\sqrt{\pi}} \int_{-\infty}^{+\infty} dk_x \exp\left[-\frac{k_x^2 \mathrm{w}_0^2}{4} + i\left(k_x x - \frac{k_x^2}{2k} z\right)\right]$$

To solve this kind of integral, the following equality demonstrated in section A.1 can be used.

$$\int_{-\infty}^{+\infty} e^{-ax^2+bx+c}\, dx = \sqrt{\frac{\pi}{a}}\ \exp\left[\frac{b^2}{4a} + c\right] \tag{2.4}$$

Using it,

$$D_x = \sqrt{\frac{1}{p}} \times \exp\left[\frac{-x^2}{\mathrm{w}_0^2\, p}\right] \tag{2.5}$$

Where

$$p = 1 + i\frac{2z}{k\mathrm{w}_0^2}$$

And therefore,

$$E(x, y, z) = E_0 \times e^{ikz} \times \frac{1}{p} \times \exp\left[\frac{-(x^2 + y^2)}{\mathrm{w}_0^2\, p}\right]$$

Knowing that the laser intensity is given by $I(x, y, z) = |E(x, y, z)|^2$,

$$I(x, y, z) = I_0 \frac{\mathrm{w}_0^2}{\mathrm{w}^2(z)} \exp\left[\frac{-2(x^2 + y^2)}{\mathrm{w}^2(z)}\right] \tag{2.6}$$

In which $\mathrm{w}(z)$ is given by

$$\mathrm{w}(z) = \mathrm{w}_0 \sqrt{1 + \left(\frac{2z}{k\mathrm{w}_0^2}\right)^2} = \mathrm{w}_0 \sqrt{1 + \left(\frac{\lambda z}{\pi \mathrm{w}_0^2}\right)^2}$$

The value $z_{\mathrm{R}} = \dfrac{\pi \mathrm{w}_0^2}{\lambda}$ is called the Rayleigh length, for which $\mathrm{w}(\pm z_{\mathrm{R}}) = \sqrt{2}\ \mathrm{w}_0$, as shown in figure 2. Hence, we have:

$$\mathrm{w}(z) = \mathrm{w}_0 \sqrt{1 + \left(\frac{z}{z_{\mathrm{R}}}\right)^2}$$

2.2 Numerical comparison

The expression for the laser intensity was obtained using series form for k_z as shown in (2.2). To verify the accuracy of the approximation, the analytical intensity is plotted and compared with points calculated numerically through *Mathematica*, as shown in figure 3. For each point, the double integral is done numerically for a specific point in space.

Note that the points land nicely on the curve for every point, showing that the expression describes well the beam behavior.

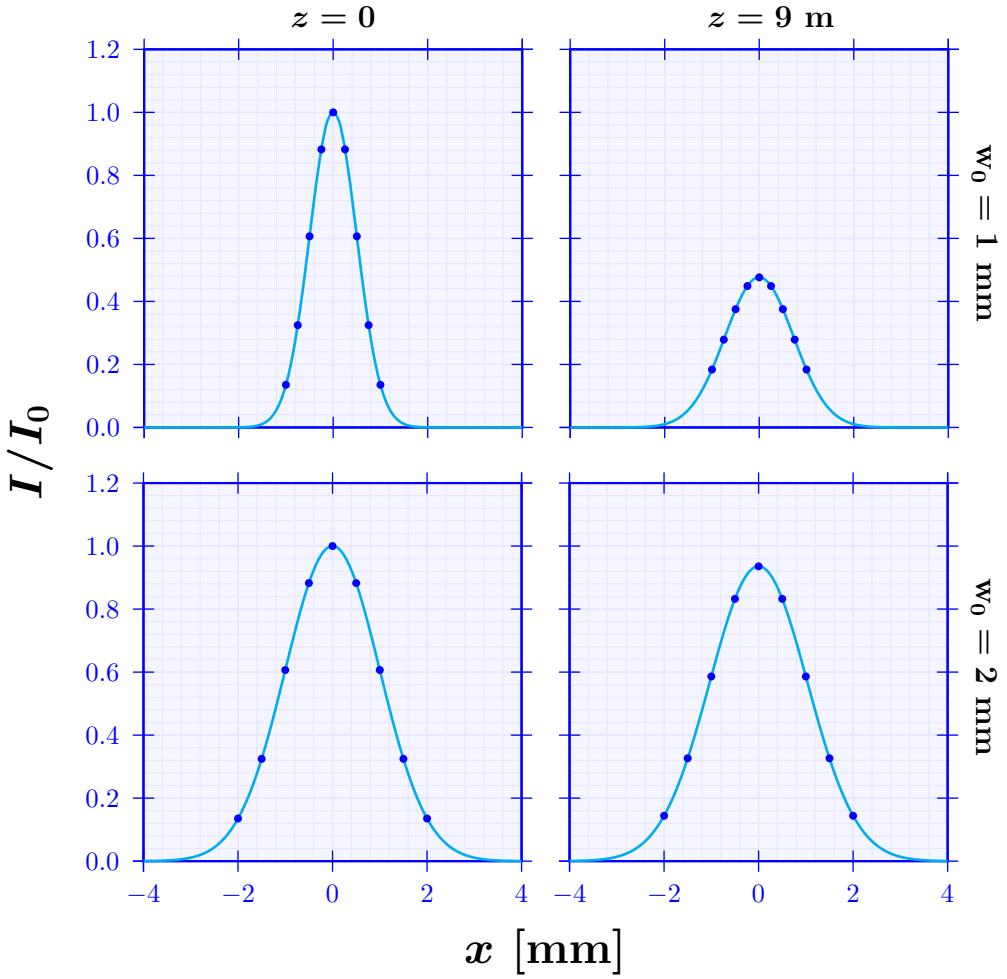

Figure 3: Comparison between analytical curves obtained for the intensity and some points obtained numerically for a laser with a $\lambda = 366$ nm wavelength on the plane $y = 0$.

3 Modified beams

To study the behavior of laser beams in situations other than free propagation, the initial model need to change. Some situations can be modeled by an addition of a linear or quadratic factor of k_x or k_y. In this secton, a factor of $(\alpha k_x + \beta k_x^2 + \gamma k_y^2)$ will be included in the electric field integral:

$$E(x,y,z) = E_0 \frac{w_0^2}{4\pi} \int_{-\infty}^{+\infty} dk_x \int_{-\infty}^{+\infty} dk_y \ (\alpha k_x + \beta k_x^2 + \gamma k_y^2) \times \exp\left[-\frac{w_0^2}{4}(k_x^2 + k_y^2)\right] \times \\ \times \exp\left[i(k_x x + k_y y + k_z z)\right]$$

3.1 Analytical development

Using again series form for k_z, we can split the equation into the following form:

$$\begin{aligned} E(x,y,z) = E_0 \times e^{ikz} \times \Bigg\{ & \frac{w_0}{2\sqrt{\pi}} \int_{-\infty}^{+\infty} dk_x \ \alpha k_x \exp\left[-\frac{k_x^2 w_0^2}{4}\right] \exp\left[i\left(k_x x - \frac{k_x^2}{2k} z\right)\right] \times \\ & \times \frac{w_0}{2\sqrt{\pi}} \int_{-\infty}^{+\infty} dk_y \ \exp\left[-\frac{k_y^2 w_0^2}{4}\right] \exp\left[i\left(k_y y - \frac{k_y^2}{2k} z\right)\right] + \\ & + \frac{w_0}{2\sqrt{\pi}} \int_{-\infty}^{+\infty} dk_x \ \beta k_x^2 \exp\left[-\frac{k_x^2 w_0^2}{4}\right] \exp\left[i\left(k_x x - \frac{k_x^2}{2k} z\right)\right] \times \\ & \times \frac{w_0}{2\sqrt{\pi}} \int_{-\infty}^{+\infty} dk_y \ \exp\left[-\frac{k_y^2 w_0^2}{4}\right] \exp\left[i\left(k_y y - \frac{k_y^2}{2k} z\right)\right] + \\ & + \frac{w_0}{2\sqrt{\pi}} \int_{-\infty}^{+\infty} dk_x \ \exp\left[-\frac{k_x^2 w_0^2}{4}\right] \exp\left[i\left(k_x x - \frac{k_x^2}{2k} z\right)\right] \times \\ & \times \frac{w_0}{2\sqrt{\pi}} \int_{-\infty}^{+\infty} dk_y \ \gamma k_y^2 \exp\left[-\frac{k_y^2 w_0^2}{4}\right] \exp\left[i\left(k_y y - \frac{k_y^2}{2k} z\right)\right] \Bigg\} \end{aligned} \tag{3.1}$$

The integral containing αk_x factor and the ones containing βk_x^2 or γk_y^2 will be solved separately to obtain the electric field E.

3.1.1 Solving the linear factor integral

$$A_x = \frac{w_0}{2\sqrt{\pi}} \int_{-\infty}^{+\infty} dk_x \ \alpha k_x \exp\left[-\frac{k_x^2 w_0^2}{4}\right] \exp\left[i\left(k_x x - \frac{k_x^2}{2k} z\right)\right] \tag{3.2}$$

This integral is similar to the ones in (2.3) and so are the formulas to solve them. The following equality is demonstrated in section A.1.

$$\int_{-\infty}^{+\infty} x e^{-ax^2+bx+c} \, dx = \left(\frac{b}{2a}\right) \sqrt{\frac{\pi}{a}} \ \exp\left[\frac{b^2}{4a} + c\right] \tag{3.3}$$

Applying (3.3) in (3.2),

$$A_x = \frac{2i\alpha x}{w_0^2 \ p} \sqrt{\frac{1}{p}} \exp\left[\frac{-x^2}{w_0^2 \ p}\right] \tag{3.4}$$

From (2.5) and (3.4),

$$A_x\ D_y = \frac{2i\alpha x}{\mathrm{w}_0^2\ p} \times \frac{1}{p} \times \exp\left[\frac{-(x^2+y^2)}{\mathrm{w}_0^2\ p}\right] \tag{3.5}$$

3.1.2 Solving the quadratic factor integral

$$B_x = \frac{\mathrm{w}_0}{2\sqrt{\pi}} \int_{-\infty}^{+\infty} dk_x\ \beta k_x^2 \exp\left[-\frac{k_x^2 \mathrm{w}_0^2}{4}\right] \exp\left[i\left(k_x x - \frac{k_x^2}{2k} z\right)\right]$$

Once again, a formula will be used to solve the integral. It is demonstrated in section A.1:

$$\int_{-\infty}^{+\infty} x^2 e^{-ax^2+bx+c}\ dx = \left(\frac{b^2+2a}{4a^2}\right)\sqrt{\frac{\pi}{a}}\ \exp\left[\frac{b^2}{4a}+c\right]$$

From it,

$$B_x = \beta\left(\frac{-x^2+\frac{\mathrm{w}_0^2}{2}p}{\frac{\mathrm{w}_0^4}{4}p^2}\right)\sqrt{\frac{1}{p}}\exp\left[\frac{-x^2}{\mathrm{w}_0^2\ p}\right] \tag{3.6}$$

From (2.5) and (3.6),

$$B_x\ D_y = \beta\left(\frac{-x^2+\frac{\mathrm{w}_0^2}{2}p}{\frac{\mathrm{w}_0^4}{4}p^2}\right) \times \frac{1}{p} \times \exp\left[\frac{-(x^2+y^2)}{\mathrm{w}_0^2\ p}\right] \tag{3.7}$$

Equivalently,

$$B_y = \frac{\mathrm{w}_0}{2\sqrt{\pi}} \int_{-\infty}^{+\infty} dk_y\ \gamma k_y^2 \exp\left[-\frac{k_y^2 \mathrm{w}_0^2}{4}\right] \exp\left[i\left(k_y y - \frac{k_y^2}{2k} z\right)\right] = \gamma\left(\frac{-y^2+\frac{\mathrm{w}_0^2}{2}p}{\frac{\mathrm{w}_0^4}{4}p^2}\right)\sqrt{\frac{1}{p}}\exp\left[\frac{-y^2}{\mathrm{w}_0^2\ p}\right]$$

And

$$D_x\ B_y = \gamma\left(\frac{-y^2+\frac{\mathrm{w}_0^2}{2}p}{\frac{\mathrm{w}_0^4}{4}p^2}\right) \times \frac{1}{p} \times \exp\left[\frac{-(x^2+y^2)}{\mathrm{w}_0^2\ p}\right] \tag{3.8}$$

3.1.3 Electric Field and Intensity

With the values obtained in equations (3.5), (3.7) and (3.8), we can get to an expression for the electric field. From (3.1), we can write:

$$E(x,y,z) = E_0 \times e^{ikz} \times (A_x \cdot D_y + B_x \cdot D_y + D_x \cdot B_y)$$

Substituting the expressions and simplifying:

$$E(x,y,z) = E_0 \times e^{ikz} \frac{2}{\mathrm{w}_0^2\ p^2} \exp\left[\frac{-(x^2+y^2)}{\mathrm{w}_0^2\ p}\right]\left[\beta+\gamma+ix\alpha - \frac{2}{\mathrm{w}_0^2\ p}(\beta x^2+\gamma y^2)\right]$$

The intensity once again is given by $I(x,y,z) = |E(x,y,z,t)|^2$.

$$\begin{aligned} I(x,y,z) = I_0 \times \exp\left[\frac{-2(x^2+y^2)}{\mathrm{w}^2(z)}\right] \times \frac{4}{\mathrm{w}^4(z)} \times \\ \times \left[\left(\beta+\gamma-\frac{2(\beta x^2+\gamma y^2)}{\mathrm{w}^2(z)}\right)^2 + \left(x\alpha + \frac{2(\beta x^2+\gamma y^2)}{\mathrm{w}^2(z)}\frac{z}{z_{\mathrm{R}}}\right)^2\right] \end{aligned} \tag{3.9}$$

3.2 Numerical comparison

Once again, comparing the results with numerical simulations done on *Mathematica*:

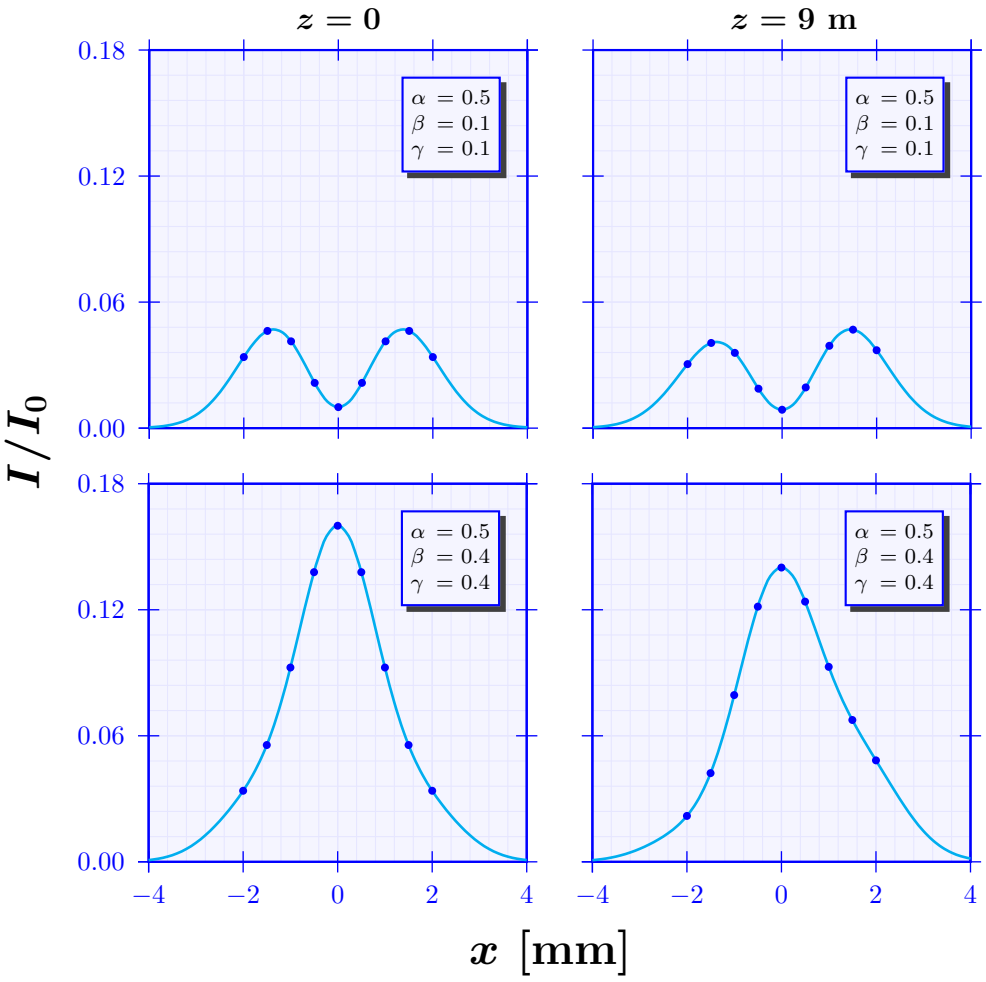

Figure 4: Comparison between analytical curves for intensity and some points obtained numerically for a laser with a $\lambda = 366$ nm wavelength and a waist of $w_0 = 2$ mm on the plane $y = 0$.

4 Laser refraction

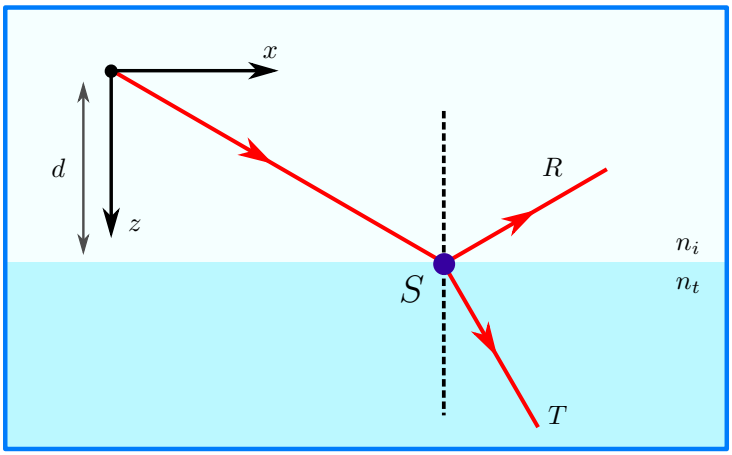

Figure 5: Plane of incidence of a laser refraction. n_i and n_t are the refractive index for the incident and transmitted media. In this example, $n_t > n_i$, but the mathematical development is valid for both cases.

In this section, the refraction of a laser in a surface dividing two media will be studied. The phenomena generates two other beams: the reflected and the transmitted.

As shown in figure 5, it is convenient to use a reference frame such that one of the axis is perpendicular to the interface. That's because the wave is affected only in the z direction when going through the interface. As changing environment affects only the z component, the electric fields can be written as

$$\begin{aligned} \text{Incident:} \quad & E_i = \exp\left[i(p_x x + p_y y + p_z z)\right] \\ \text{Reflected:} \quad & E_r = R\exp\left[i(p_x x + p_y y - p_z z)\right] \\ \text{Transmitted:} \quad & E_t = T\exp\left[i(p_x x + p_y y + q_z z)\right] \end{aligned}$$

From $B = (n/c_0)E$, where c_0 is light speed in vacuum, the magnetic field B can be derived:

$$\begin{aligned} B_i &= (n_i/c_0)\ \exp\left[i(p_x x + p_y y + p_z z)\right] \\ B_r &= (n_i/c_0)\ R\exp\left[i(p_x x + p_y y - p_z z)\right] \\ B_t &= (n_t/c_0)\ T\exp\left[i(p_x x + p_y y + q_z z)\right] \end{aligned}$$

The boundary conditions ensure that the components of the electric and magnetic fields parallel to the surface should be continuous. [2] Therefore, the coefficients R and T depend on the polarization of the laser.

4.1 Transverse electric polarization

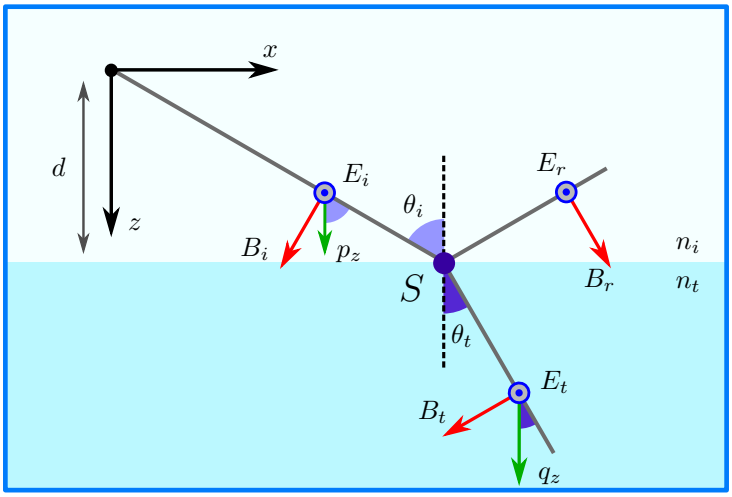

Figure 6: Plane of incidence of a laser refraction for transverse electric polarization. The electric field E is represented in blue and the magnetic B in red. The wave vectors in the z direction are in green.

Consider a **s-polarized** beam i.e. the electric field lies in the y direction, as shown in figure 6. As said, the electric and magnetic field parallel to the surface are continuous. This allows to write

$$\begin{cases} E_i + E_r = E_t \\ -B_i \cos\theta_i + B_r \cos\theta_i = -B_t \cos\theta_t \end{cases} \tag{4.1}$$

Note from figure 6 that

$$p_z = n_i k \cos\theta_i \rightarrow cos\theta_i = \frac{p_z}{n_i k}$$
$$q_z = n_t k \cos\theta_t \rightarrow cos\theta_t = \frac{q_z}{n_t k}$$

Substituting our equations into (4.1),

$$\begin{cases} \exp[ip_z z] + R^{[TE]} \exp[-ip_z z] = T^{[TE]} \exp[iq_z z] \\ p_z \Big(\exp[ip_z z] + R^{[TE]} \exp[-ip_z z] \Big) = q_z \; T^{[TE]} \exp[iq_z z] \end{cases}$$

Solving the system for $R^{[TE]}$ and $T^{[TE]}$ at $z = d$,

$$\begin{aligned} R^{[TE]} &= \frac{p_z - q_z}{p_z + q_z} \exp[2i \cdot p_z d] \\ T^{[TE]} &= \frac{2p_z}{p_z + q_z} \exp[i \cdot (p_z - q_z) d] \end{aligned} \tag{4.2}$$

Note that these relations are the **Fresnel equations** for s-polarized light.

4.2 Transverse magnetic polarization

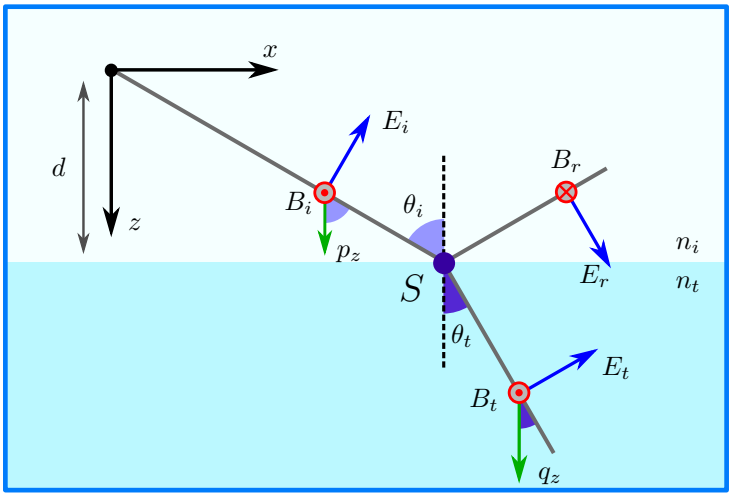

Figure 7: Plane of incidence of a laser refraction for transverse magnetic polarization. The electric field E is represented in blue and the magnetic B in red. The wave vectors in the z direction are in green.

For a **p-polarized** beam, the electric field lies in the plane of incidence, perpendicular to the wave vector, as shown in figure 7. In this case, the continuity equations give

$$\begin{cases} E_i \cos\theta_i + E_r \cos\theta_i = E_t \cos\theta_t \\ B_i - B_r = B_t \end{cases}$$

And consequently

$$\begin{cases} \dfrac{p_z}{n_i}\Big(\exp\left[ip_z z\right] + R^{[TM]} \exp\left[-ip_z z\right]\Big) = \dfrac{q_z}{n_t}\, T^{[TM]} \exp\left[iq_z z\right] \\ n_i\Big(\exp\left[ip_z z\right] - R^{[TM]} \exp\left[-ip_z z\right]\Big) = n_t\, T^{[TM]} \exp\left[iq_z z\right] \end{cases}$$

Solving the system for $z = d$ leads to:

$$\begin{aligned} R^{[TM]} &= \frac{n_t^2\, p_z - n_i^2\, q_z}{n_t^2\, p_z + n_i^2\, q_z} \exp\left[2i \cdot p_z d\right] \\ T^{[TM]} &= \frac{2p_z\, n_i n_t}{n_t^2\, p_z + n_i^2\, q_z} \exp\left[i \cdot (p_z - q_z) d\right] \end{aligned} \tag{4.3}$$

These formulas are the **Fresnel equations** for p-polarized light.

5 Laser interaction with dielectric prism

The general refraction formulas will now be used to analyze the interactions between an incident beam and a prism as shown in figure 8. The laser will go through 3 interactions with the interfaces.

As done in the section 4, on each interaction it is convenient to use a referential such that one of the axes is perpendicular to the interface. Figure 9 illustrates the three references used to analyze the refractions.

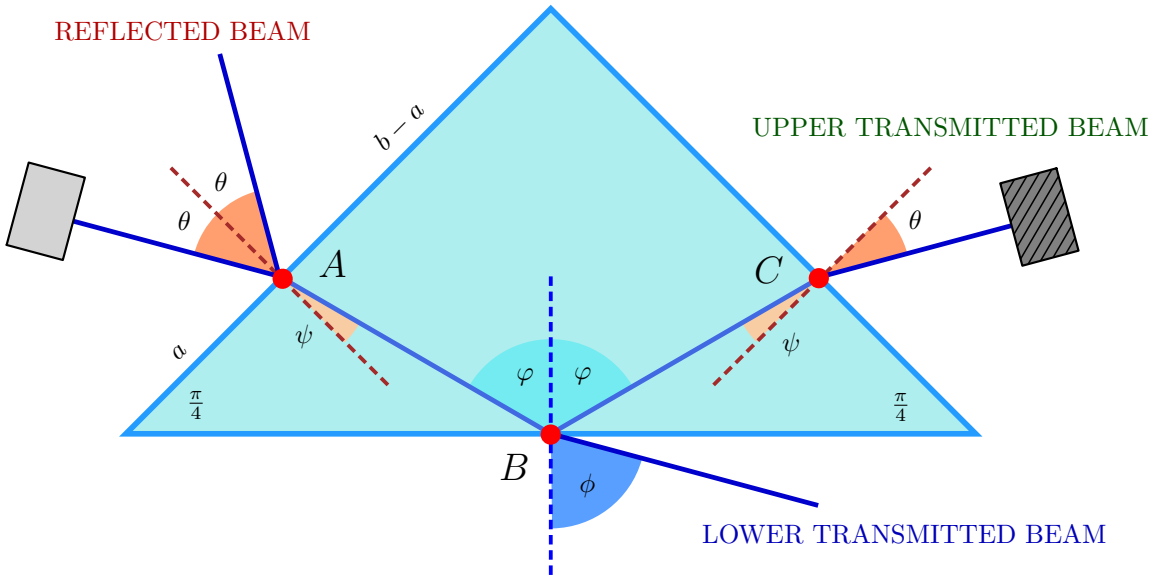

Figure 8: Plane of incidence of the dielectric prism, where all the interactions occur.

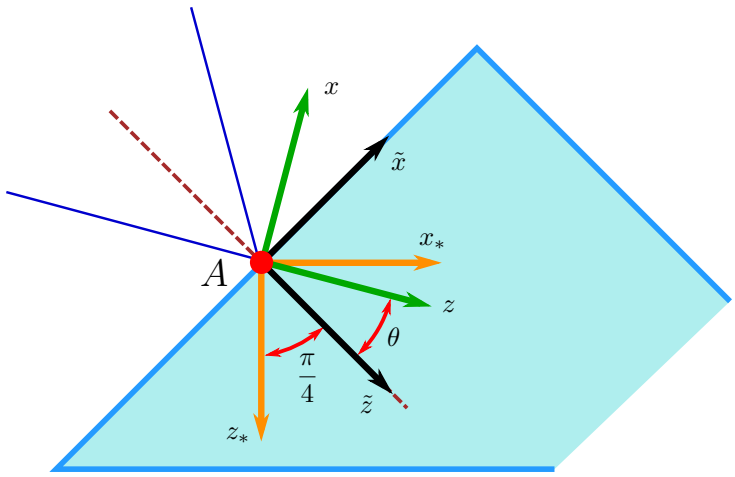

Figure 9: Reference frames used to analyze the interactions. In green, (x, z), where z is the direction of propagation of the incident beam. In black, $(\tilde{x}, \tilde{z})$, a rotation by θ of (x, z), used to analyze the interactions at A and C. In orange, (x_*, z_*), a rotation by $\pi/4$ of $(\tilde{x}, \tilde{z})$, used to analyze the interaction at B.

5.1 Interaction at A

Inside the prism, the wave speed is modified by a factor of $1/n$, such that the new wave number is nk and consequently:

$$(nk)^2 = k_{\tilde{x}}^2 + k_y^2 + q_{\tilde{z}}^2$$

$$q_{\tilde{z}} = \sqrt{(n^2-1)k^2 + k_{\tilde{z}}^2} \tag{5.1}$$

Knowing that $k_{\tilde{x}}$ and $k_{\tilde{z}}$ are just the rotation of k_x and k_z, they can be expressed using a rotation matrix as in (5.2). The approximation $k_z \approx k$ is used here as z is the propagation direction of the incident beam.

$$\begin{pmatrix} \tilde{x} \\ \tilde{z} \end{pmatrix} = \begin{pmatrix} \cos\theta & \sin\theta \\ -\sin\theta & \cos\theta \end{pmatrix} \cdot \begin{pmatrix} x \\ z \end{pmatrix} \tag{5.2}$$

$$k_{\tilde{x}} = k_x \cos\theta + k_z \sin\theta \approx k_x \cos\theta + k \sin\theta \tag{5.3}$$

$$k_{\tilde{z}} = k_z \cos\theta - k_x \sin\theta \approx k \cos\theta - k_x \sin\theta \tag{5.4}$$

As the laser collides with the first prism surface, two new beams are formed, as show in figure 8. The reflected and transmitted waves are

$$\begin{aligned} \text{Reflected:} \quad & R_{_A} \exp\left[i(k_{\tilde{x}}\tilde{x} + k_y y - k_{\tilde{z}}\tilde{z})\right] \\ \text{Transmitted:} \quad & T_{_A} \exp\left[i(k_{\tilde{x}}\tilde{x} + k_y y + q_{\tilde{z}}\tilde{z})\right] \end{aligned}$$

Applying (4.2) and (4.3):

$$R_{_A}^{[TE]} = \frac{k_{\tilde{z}} - q_{\tilde{z}}}{k_{\tilde{z}} + q_{\tilde{z}}}, \; T_{_A}^{[TE]} = \frac{2k_{\tilde{z}}}{k_{\tilde{z}} + q_{\tilde{z}}}$$

$$R_{_A}^{[TM]} = \frac{n^2 k_{\tilde{z}} - q_{\tilde{z}}}{n^2 k_{\tilde{z}} + q_{\tilde{z}}}, \; T_{_A}^{[TM]} = \frac{2k_{\tilde{z}} n}{n^2 k_{\tilde{z}} + q_{\tilde{z}}}$$

5.2 Interaction at B

For the second interface, the (x_*, z_*) referential will be used, as z_* is perpendicular to the face. The incident beam (from A) can be wrote in terms of q_{x_*} and q_{z_*} with a rotation by $\pi/4$ clockwise. From that, we can obtain the values of q_{x_*} and q_{z_*}:

$$\begin{pmatrix} x_* \\ z_* \end{pmatrix} = \begin{pmatrix} \cos(\pi/4) & \sin(\pi/4) \\ -\sin(\pi/4) & \cos(\pi/4) \end{pmatrix} \cdot \begin{pmatrix} \tilde{x} \\ \tilde{z} \end{pmatrix} = \frac{1}{\sqrt{2}} \begin{pmatrix} 1 & 1 \\ -1 & 1 \end{pmatrix} \cdot \begin{pmatrix} \tilde{x} \\ \tilde{z} \end{pmatrix} \tag{5.5}$$

$$q_{x_*} = \frac{1}{\sqrt{2}}(q_{\tilde{z}} + k_{\tilde{x}})$$

$$q_{z_*} = \frac{1}{\sqrt{2}}(q_{\tilde{z}} - k_{\tilde{x}}) \tag{5.6}$$

For the transmitted beam, once again the only component that changes is in the z_* direction:

$$k^2 = q_{x_*}^2 + k_y^2 + k_{z_*}^2$$

$$k_{z_*} = \sqrt{(1-n^2)k^2 + q_{z_*}^2} \tag{5.7}$$

The reflected and transmitted waves can be described by:

$$\begin{aligned} \text{Reflected:} \quad & R_{_B} \exp\left[i(q_{x_*}x_* + k_y y - q_{z_*}z_*)\right] \\ \text{Transmitted:} \quad & T_{_B} \exp\left[i(q_{x_*}x_* + k_y y + k_{z_*}z_*)\right] \end{aligned}$$

To determine the coefficients $R_{_B}$ and $T_{_B}$, the refraction formulas (4.2) and (4.3) are used once again:

$$R_{_B}^{[TE]} = \frac{q_{z_*} - k_{z_*}}{q_{z_*} + k_{z_*}} \exp\left[2i \cdot q_{z_*} \frac{a}{\sqrt{2}}\right], \; T_{_B}^{[TE]} = \frac{2q_{z_*}}{q_{z_*} + k_{z_*}} \exp\left[i \cdot (q_{z_*} - k_{z_*}) \frac{a}{\sqrt{2}}\right] \tag{5.8}$$

$$R_{_B}^{[TM]} = \frac{q_{z_*} - n^2 k_{z_*}}{q_{z_*} + n^2 k_{z_*}} \exp\left[2i \cdot q_{z_*} \frac{a}{\sqrt{2}}\right], \; T_{_B}^{[TM]} = \frac{2q_{z_*}\, n}{q_{z_*} + n^2 k_{z_*}} \exp\left[i \cdot (q_{z_*} - k_{z_*}) \frac{a}{\sqrt{2}}\right] \tag{5.9}$$

5.3 Interaction at C

To write the BC beam in $(\tilde{x}, \tilde{z})$ coordinates, as shown in figure 10, note that the angle between the laser and the $\tilde{x}$ axis is ϕ, the same angle between the AB beam and the $\tilde{z}$ axis. Furthermore, both components of the BC laser must be positive, the same case from AB beam. This allows to rewrite the incident laser at C as:

$$\text{Incident: } \exp\left[i(q_{\tilde{z}}\tilde{x} + k_y y + k_{\tilde{x}}\tilde{z})\right]$$

This time, the wave number will change in the $\tilde{x}$ direction, while $k_{\tilde{x}}$ remains the same outside of the prism. Therefore,

$$\text{Transmitted: } T_{_C} \exp\left[i(k_{\tilde{z}}\tilde{x} + k_y y + k_{\tilde{x}}\tilde{z})\right] \tag{5.10}$$

Finally, by (4.2) and (4.3),

$$T_{_C}^{[TE]} = \frac{2\ q_{\tilde{z}}}{q_{\tilde{z}} + k_{\tilde{z}}} \exp\left[i \cdot (q_{\tilde{z}} - k_{\tilde{z}})(b-a)\right] \tag{5.11}$$

$$T_{_C}^{[TM]} = \frac{2q_{\tilde{z}}\ n}{q_{\tilde{z}} + n^2 k_{\tilde{z}}} \exp\left[i \cdot (q_{\tilde{z}} - k_{\tilde{z}})(b-a)\right] \tag{5.12}$$

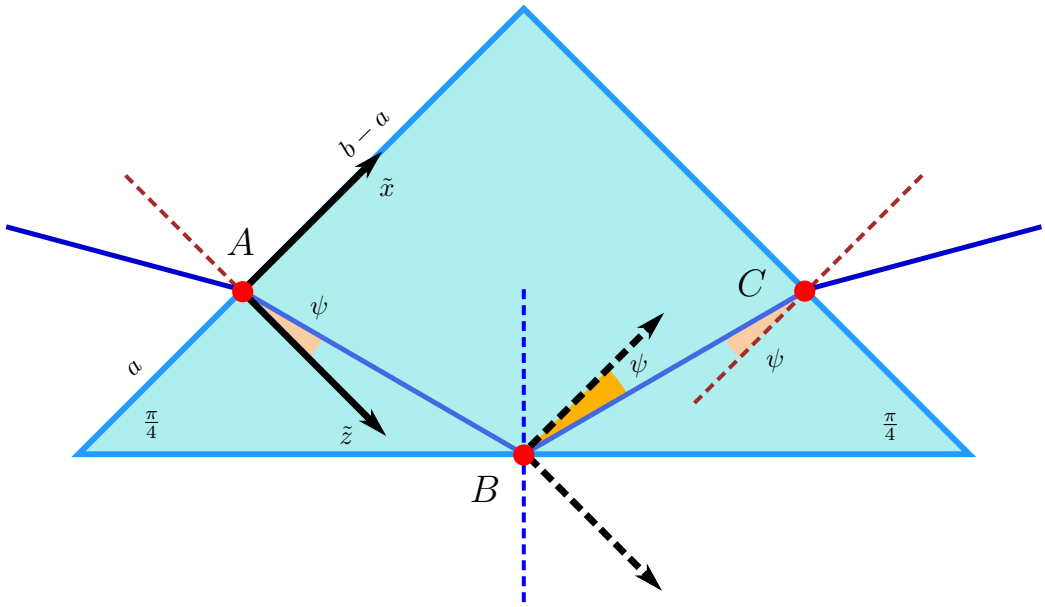

Figure 10: Plane of incidence of the prism, with projection of $(\tilde{x}, \tilde{z})$ reference frame to point B to show that the angle between the BC beam and the $\tilde{x}$ axis is ψ.

6 Transmitted beam path

A new reference frame $(x_{\text{TRA}}, z_{\text{TRA}})$ is convenient to study the upper transmitted beam, with origin in A and z_{TRA} in the direction of propagation of the laser. As shown in figure 11, $(x_{\text{TRA}}, z_{\text{TRA}})$ is the rotation of $(\tilde{x}, \tilde{z})$ by $\pi/2 - \theta$ clockwise.

$$\begin{pmatrix} x_{\text{TRA}} \\ z_{\text{TRA}} \end{pmatrix} = \begin{pmatrix} \cos(\pi/2-\theta) & -\sin(\pi/2-\theta) \\ \sin(\pi/2-\theta) & \cos(\pi/2-\theta) \end{pmatrix} \cdot \begin{pmatrix} \tilde{x} \\ \tilde{z} \end{pmatrix} = \begin{pmatrix} \sin\theta & -\cos\theta \\ \cos\theta & \sin\theta \end{pmatrix} \cdot \begin{pmatrix} \tilde{x} \\ \tilde{z} \end{pmatrix} \tag{6.1}$$

The transmitted beam, therefore, is given by

$$T_A R_B T_C \exp\left[i(-k_x x_{\text{TRA}} + k_y y + k_z z_{\text{TRA}})\right] \tag{6.2}$$

The distance d will be determine by two separated ways. First, geometry will be used along with Snell's law. Next, it will be discussed how to get to d using the beam's phase and then compare the results obtained.

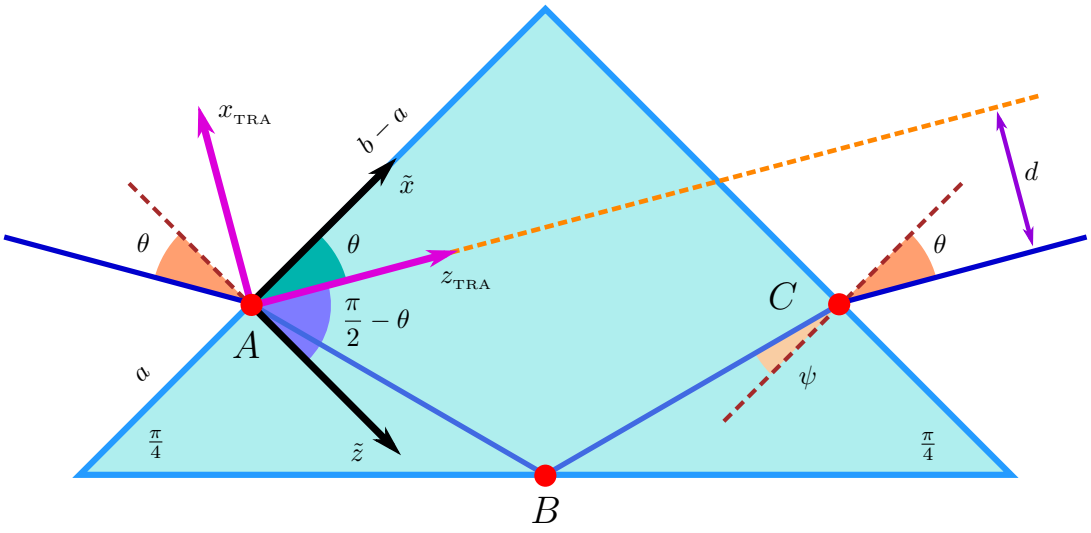

Figure 11: Plane of incidence of the prism, with new reference frame $(x_{\text{TRA}}, z_{\text{TRA}})$, a rotation by $\pi/2 - \theta$ of $(\tilde{x}, \tilde{z})$ counterclockwise. The projection of z_{TRA} axis shows that the transmitted beam is at $x_{\text{TRA}} = -d$.

6.1 Upper transmitted beam path using geometry

Note that $d = -x_{\text{TRA}}(C)$. To ease the calculation of C coordinates, (x_*, z_*) referential is useful here, as shown in figure 12. From the image,

$$\tan(\psi + \pi/4) = \frac{x_*(C)}{a\sqrt{2} - z_*(C)}$$

And

$$x_*(C) = (b-a)\sqrt{2} + z_*(C)$$

These two equations form a two variable system, with solution:

$$x_*(C) = \sqrt{2}\left(b - \frac{b}{2}(1 - \tan\psi)\right) \tag{6.3}$$

$$z_*(C) = \sqrt{2}\left(a - \frac{b}{2}(1 - \tan\psi)\right) \tag{6.4}$$

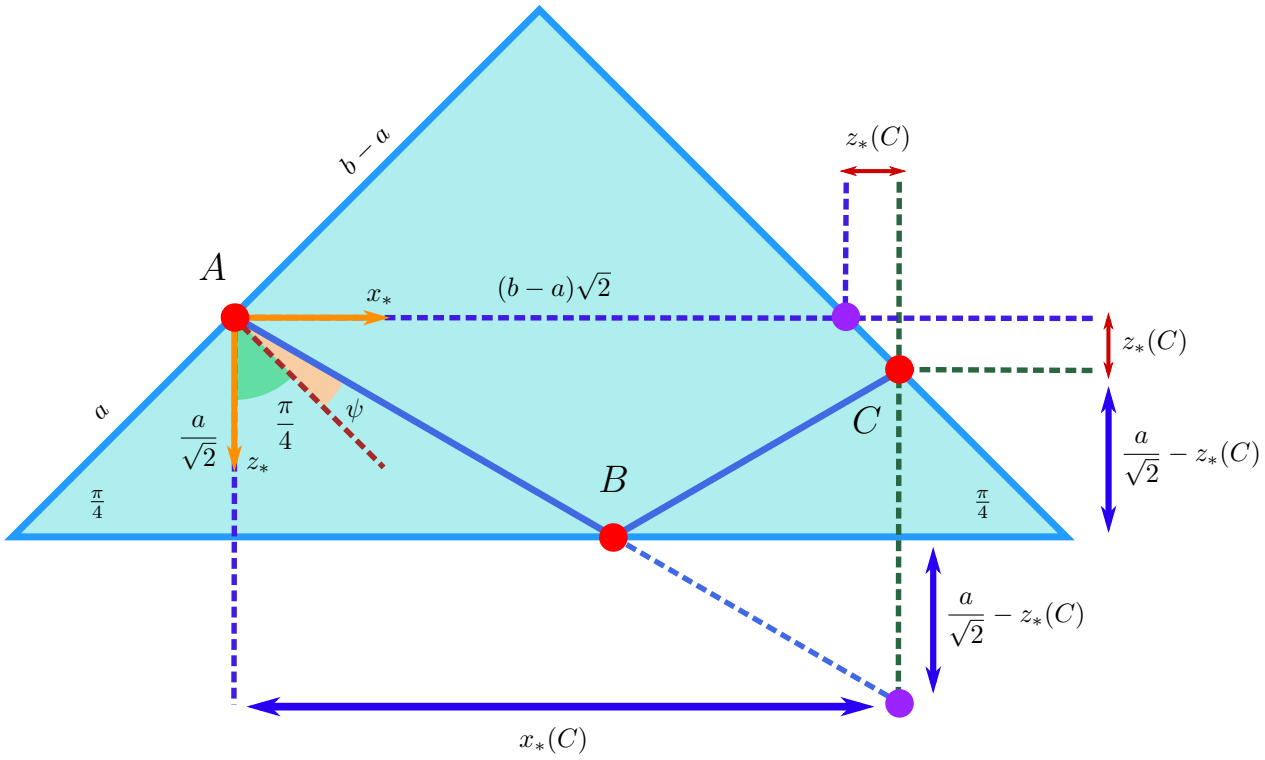

Figure 12: Plane of incidence of the prism with reference (x_*, z_*) and some distances useful for the calculation of d.

Note from (5.5) that

$$\begin{pmatrix} \tilde{x} \\ \tilde{z} \end{pmatrix} = \frac{1}{\sqrt{2}} \begin{pmatrix} 1 & -1 \\ 1 & 1 \end{pmatrix} \cdot \begin{pmatrix} x_* \\ z_* \end{pmatrix}$$

And therefore, from (6.1):

$$\begin{pmatrix} x_{\text{TRA}} \\ z_{\text{TRA}} \end{pmatrix} = \frac{1}{\sqrt{2}} \begin{pmatrix} \sin\theta & -\cos\theta \\ \cos\theta & \sin\theta \end{pmatrix} \cdot \begin{pmatrix} 1 & -1 \\ 1 & 1 \end{pmatrix} \cdot \begin{pmatrix} x_* \\ z_* \end{pmatrix} = \frac{1}{\sqrt{2}} \begin{pmatrix} \sin\theta - \cos\theta & -\sin\theta - \cos\theta \\ \sin\theta + \cos\theta & \sin\theta - \cos\theta \end{pmatrix} \cdot \begin{pmatrix} x_* \\ z_* \end{pmatrix}$$

Now, it's possible to get $x_{\text{TRA}}(C)$:

$$x_{\text{TRA}}(C) = \frac{x_*(C)}{\sqrt{2}}(\sin\theta - \cos\theta) + \frac{z_*(C)}{\sqrt{2}}(-\sin\theta - \cos\theta)$$

And d:

$$d = -x_{\text{TRA}}(C) = (a + b\tan\psi)\cos\theta + (a - b)\sin\theta$$

From Snell's law, $\sin\theta = n\sin\psi$. After some work,

$$\tan\psi = \frac{\sin\theta}{\sqrt{n^2 - \sin^2\theta}}$$

And finally

$$d = \left[a + \frac{\sin\theta}{\sqrt{n^2 - \sin^2\theta}} \cdot b\right]\cos\theta + (a - b)\sin\theta$$

6.2 Upper transmitted beam path using series form

Now the path of the transmitted beam will be derived by the analysis of its phase, which is the combination of the phase factors in T_A, R_B and T_C. The phases from (5.8), (5.11) and (6.2) combined give the beam total phase:

$$k_{\tilde{z}}\tilde{x} + k_y y + k_{\tilde{x}}\tilde{z} + \gamma$$

Where

$$\gamma = q_{z_*} a\sqrt{2} + (q_{\tilde{z}} - k_{\tilde{z}})(b - a)$$

In this phase, the coefficient of k_x in γ gives the lateral displacement, once it can be identified in (6.2) as a translation of x_{TRA}:

$$-k_x(x_{\text{TRA}} + d)$$

A approximation for d will be obtained expanding γ to first order w.r.t. k_x:

$$\gamma(k_x) \approx \gamma(0) + \left.\frac{\partial\gamma}{\partial k_x}\right|_0 \cdot k_x$$

With this form, it's easy to note that

$$d = -\left.\frac{\partial\gamma}{\partial k_x}\right|_0 \tag{6.5}$$

Now remains the calculation of the partial derivatives of the wave components involved. From (5.3) and (5.4):

$$\frac{\partial k_{\tilde{x}}}{\partial k_x} = \cos\theta, \quad \frac{\partial k_{\tilde{z}}}{\partial k_x} = -\sin\theta$$

From (5.1):

$$\frac{\partial q_{\tilde{z}}}{\partial k_x} = \frac{\partial q_{\tilde{z}}}{\partial k_{\tilde{z}}}\frac{\partial k_{\tilde{z}}}{\partial k_x} = -\frac{k_{\tilde{z}}}{q_{\tilde{z}}}\sin\theta$$

From (5.6):

$$\frac{\partial q_{z_*}}{\partial k_x} = \frac{1}{\sqrt{2}}\left(\frac{\partial q_{\tilde{z}}}{\partial k_x} - \frac{\partial q_{\tilde{x}}}{\partial k_x}\right) = -\frac{1}{\sqrt{2}}\left(\frac{k_{\tilde{z}}\sin\theta + q_{\tilde{z}}\cos\theta}{q_{\tilde{z}}}\right)$$

Now, solving (6.5),

$$d = \left[a + \frac{\sin\theta}{\sqrt{n^2 - \sin^2\theta}} \cdot b\right]\cos\theta + (a - b)\sin\theta$$

The exact result derived from geometry with Snell's law. Thus, in the case where the laser goes through **partial internal reflection** in B, this method results in the same conclusions as the use of geometry.

6.3 Numerical comparison

The analytical result obtained in both methods can be compared to numerical simulations performed in *Mathematica*, as shown in figure 13.

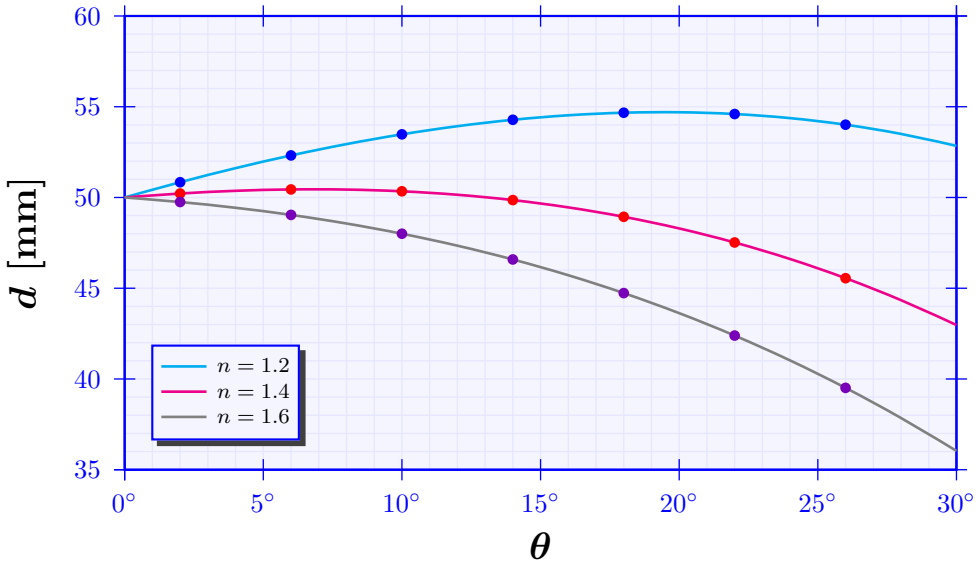

Figure 13: Lateral shift d for a prism with dimensions $a = 5$ cm and $b = 15$ cm for different refractive indexes. The lines represent the analytical results and the dots represent values from simulations.

7 Goos-Hänchen effect

In point B, as the air has a refractive index smaller than the prism, the beam can arrive at the surface with an incident angle θ greater than critical angle θ_c and reflect completely. In this case of **total internal reflection**, k_{z_*} is a complex value, as (5.7) shows. In this case, therefore, there is an additional phase δ from the complex coefficient of $R_{_B}$ in (5.8) or (5.9). This change will cause a shift Δ in the path of the outgoing beam, known as Goos-Hänchen shift. [3] The change in d will depend on the polarization of the laser.

7.1 Transverse electric polarization

As k_{z_*} is purely imaginary, for a s-polarized beam, the $R_{_B}^{[TE]}$ coefficient can be written as

$$\frac{q_{z_*} - i|k_{z_*}|}{q_{z_*} + i|k_{z_*}|} = \frac{(q_{z_*} - i|k_{z_*}|)^2}{q_{z_*}^2 + |k_{z_*}|^2}$$

The phase $\delta^{[TE]}$ can be extracted:

$$\tan\left(2\delta^{[TE]}\right) = -\frac{|k_{z_*}|}{q_{z_*}} \rightarrow \delta^{[TE]} = -2\arctan\left(\frac{|k_{z_*}|}{q_{z_*}}\right)$$

After some work,

$$\frac{\partial\delta^{[TE]}}{\partial k_x} = \frac{-2}{q_{z_*}^2 + |k_{z_*}|^2}\left(q_{z_*}\frac{\partial|k_{z_*}|}{\partial k_x} - |k_{z_*}|\frac{\partial q_{z_*}}{\partial k_x}\right)$$

Note from (5.7) that in this case

$$|k_{z_*}| = \sqrt{(n^2-1)k^2 - q_{z_*}^2}$$

Consequently,

$$q_{z_*}^2 + |k_{z_*}|^2 = (n^2-1)k^2$$

And

$$\frac{\partial|k_{z_*}|}{\partial k_x} = -\frac{q_{z_*}}{|k_{z_*}|}\frac{\partial q_{z_*}}{\partial k_x}$$

Using the derivatives relations from last section,

$$\frac{\partial\delta^{[TE]}}{\partial k_x} = \frac{2}{|k_{z_*}|}\frac{\partial q_{z_*}}{\partial k_x} = \frac{2}{|k_{z_*}|}\left(-\frac{1}{\sqrt{2}}\cdot\frac{k_{\tilde{z}}\sin\theta + q_{\tilde{z}}\cos\theta}{q_{\tilde{z}}}\right)$$

Now the definition of the components can be used to calculate them with $k_x = 0$ and do some work to reach:

$$\Delta^{[TE]} = -\left.\frac{\partial\delta^{[TE]}}{\partial k_x}\right|_{k_x=0} = \frac{2\cos\theta\left(\sin\theta + \sqrt{n^2 - \sin^2\theta}\right)}{k\sqrt{\left(n^2 - 2 + 2\sin\theta\sqrt{n^2-\sin^2\theta}\right)\left(n^2-\sin^2\theta\right)}}$$

7.2 Transverse magnetic polarization

For a p-polarized beam, the $R_{_B}$ coefficient is different:

$$\frac{q_{z_*} - in^2|k_{z_*}|}{q_{z_*} + in^2|k_{z_*}|} = \frac{(q_{z_*} - i^2|k_{z_*}|)^2}{q_{z_*}^2 + n^4|k_{z_*}|^2}$$

The phase $\delta^{[TM]}$ is given by

$$\tan\left(2\delta^{[TM]}\right) = -n^2\frac{|k_{z_*}|}{q_{z_*}} \rightarrow \delta^{[TE]} = -2\arctan\left(n^2\frac{|k_{z_*}|}{q_{z_*}}\right)$$

Similarly, the derivative is calculated:

$$\begin{aligned}\frac{\partial\delta^{[TM]}}{\partial k_x} &= \frac{2n^2}{q_{z_*}^2 + n^4|k_{z_*}|^2}\cdot\frac{q_{z_*}^2 + |k_{z_*}|^2}{|k_{z_*}|}\cdot\frac{\partial q_{z_*}}{\partial k_x} \\ &= \frac{n^2k^2}{n^4k^2 - q_{z_*}^2(n^2+1)}\cdot\underbrace{\frac{2}{|k_{z_*}|}\left(-\frac{1}{\sqrt{2}}\cdot\frac{k_{\tilde{z}}\sin\theta + q_{\tilde{z}}\cos\theta}{q_{\tilde{z}}}\right)}_{\frac{\partial\delta^{[TE]}}{\partial k_x}}\end{aligned}$$

Finally,

$$\Delta^{[TM]} = -\frac{\partial\delta^{[TM]}}{\partial k_x}\bigg|_{k_x=0} = \frac{2n^2}{2n^4 - (n^2+1)\left(n^2 - 2\sin\theta\sqrt{n^2-\sin^2\theta}\right)}\cdot\Delta^{[TE]}$$

7.3 Numerical comparison

Once again, the analytical results obtained for both polarizations can be compared with numerical simulations performed in *Mathematica*. Note from figure 14 how the numerical dots match perfectly the analytical curves.

As $\theta \rightarrow {\theta_c}^+$, however, the analytical curve tends to infinity, a physical absurd. Figure 15 shows what actually happen in this region, with a smooth transition. A detailed study of an analytical expression for this region can be found in [4].

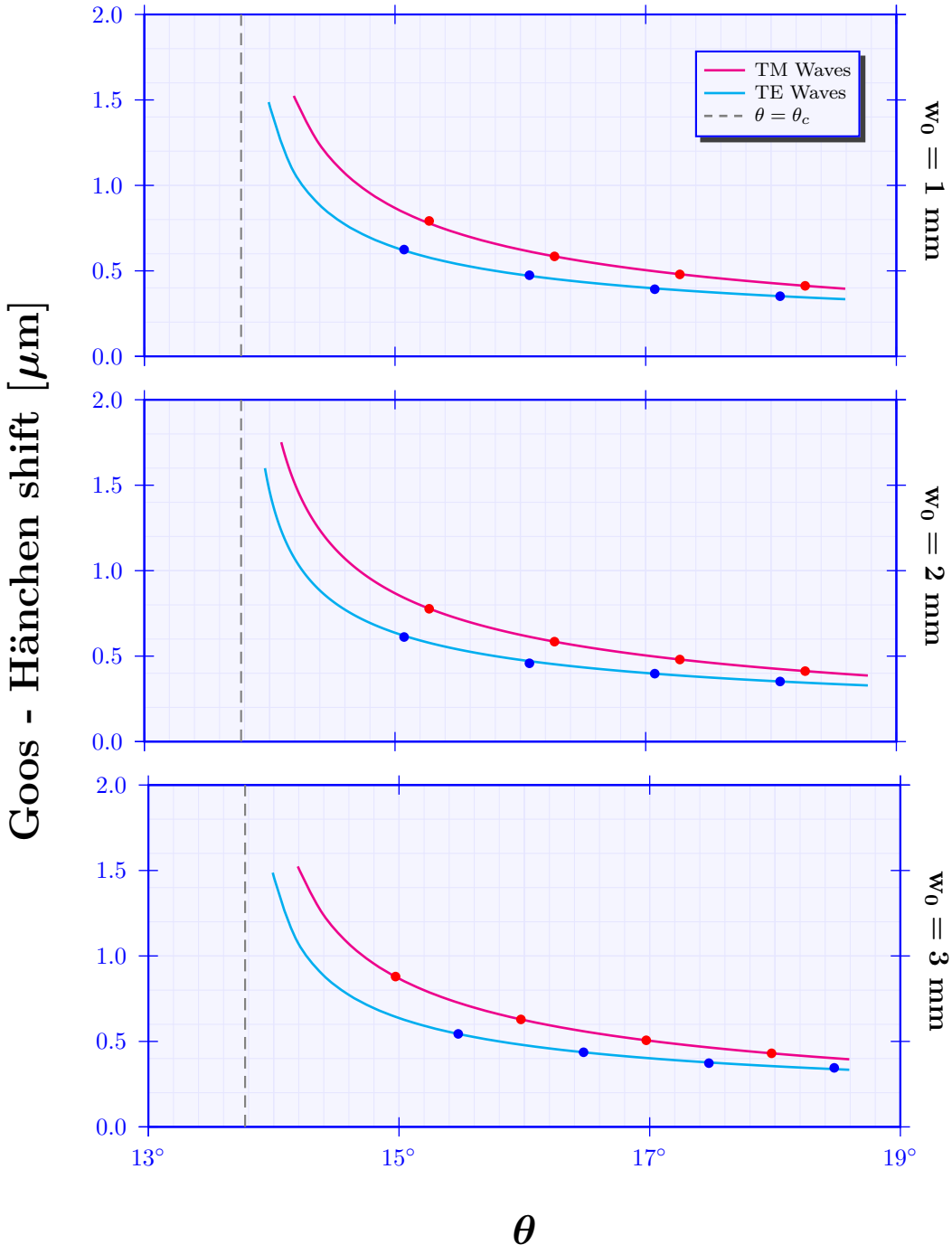

Figure 14: Goos-Hänchen shift for a material with refractive index $n = 1.2$ and a 366 nm wavelength laser. The data refers to a prism with dimensions $a = 5$ cm and $b = 15$ cm. The numerical values obtained in simulations are represented by the dots and match perfectly the analytical curves.

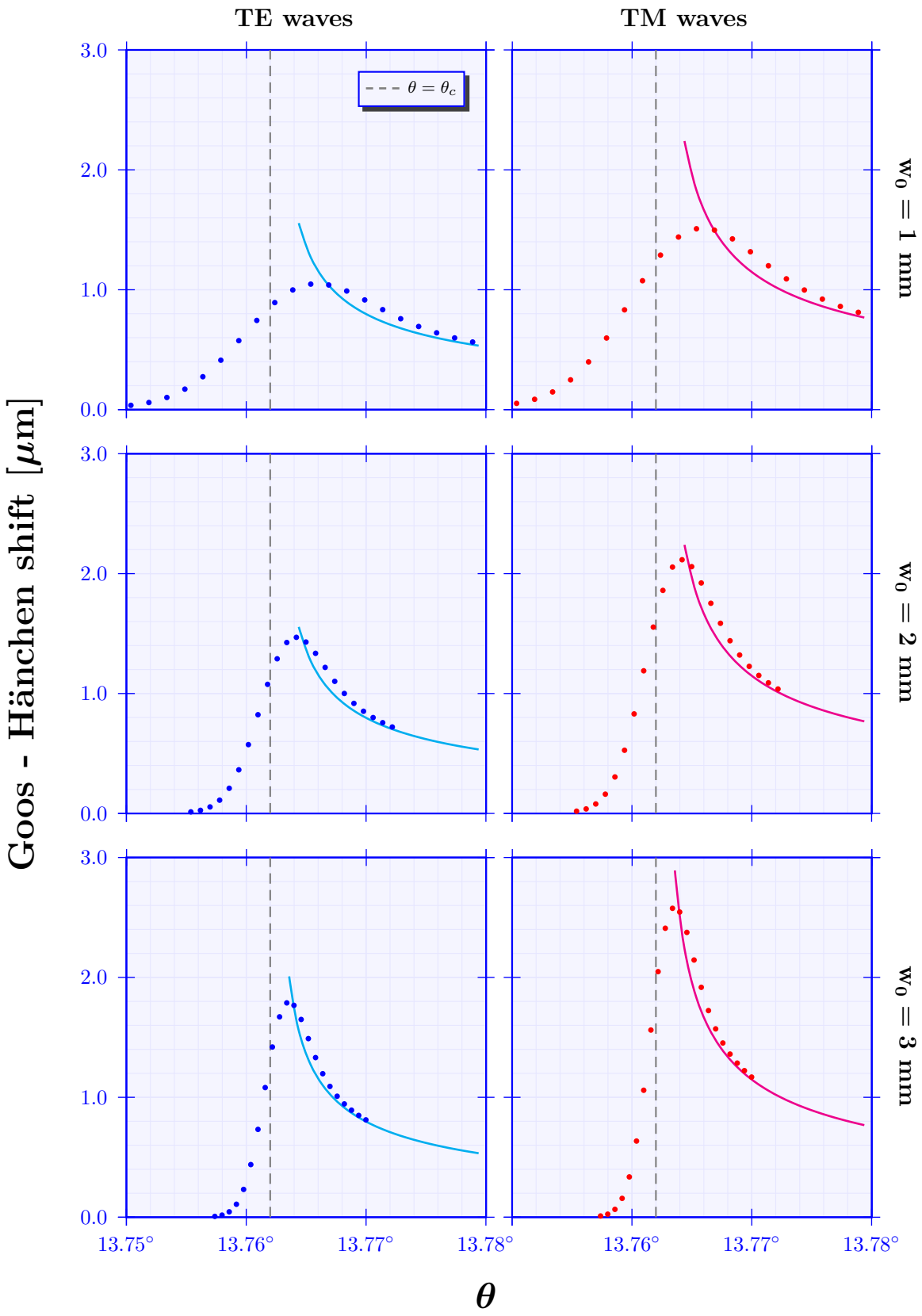

Figure 15: Goos-Hänchen shift for a material with refractive index $n = 1.2$ and a 366 nm wavelength laser. The data refers to a prism with dimensions $a = 5$ cm and $b = 15$ cm. Note that in this region, the numerical dots show the smooth transition between $\theta < \theta_c$ and $\theta > \theta_c$.

8 Conclusion

In this study, it was shown how to solve analytically the integrals for the electric field of a Gaussian beam laser, in both cases of free propagation and behavior modified by a media. The analytical intensity obtained from the electric field was compared to numerical values, ensuring that the approximation to the first order of k_z is enough to get consistent results with the formula.

After that, Fresnel equations for refraction were derived from the boundary conditions at a discontinuity interface. The method used include not only the amplitude coefficients, but also the the wave phase, making possible the use of the results to determine a beam path by expanding the phase in series form, as in section 6. This path was also determined using Snell's law and some geometry, resulting in the same expression.

Finally, the Goos-Hänchen effect was explored. The series form to first order of the laser phase was used to reach analytical expressions for the lateral shift. These formula perfectly matched the numerical values, except in the critical region around $\theta = \theta_c$. Therefore, the expressions presented are a great approximation of the laser out this tiny area.

An article to be published soon will use this study as a base.

A Demonstrations

A.1 Quadratic exponential integrals

Formula for simple quadratic exponential integrals:

$$\int_{-\infty}^{+\infty} e^{-ax^2+bx+c}\,dx = \sqrt{\frac{\pi}{a}}\,\exp\left[\frac{b^2}{4a}+c\right]$$

Proof.

$$\begin{aligned}
\int_{-\infty}^{+\infty} e^{-ax^2+bx+c}\,dx &= \int_{-\infty}^{+\infty} \exp\left[-a\left(x^2-\frac{b}{a}x+\frac{b^2}{4a^2}-\frac{b^2}{4a^2}-\frac{c}{a}\right)\right]dx \\
&= \int_{-\infty}^{+\infty} \exp\left[-a\left(\left(x-\frac{b}{2a}\right)^2-\frac{b^2}{4a^2}-\frac{c}{a}\right)\right]dx \\
&= \exp\left[\frac{b^2}{4a}+c\right]\int_{-\infty}^{+\infty} \exp\left[-a\left(x-\frac{b}{2a}\right)^2\right]dx \\
&= \exp\left[\frac{b^2}{4a}+c\right]\int_{-\infty}^{+\infty} \exp\left[-at^2\right]dt \\
&= \sqrt{\frac{\pi}{a}}\,\exp\left[\frac{b^2}{4a}+c\right]
\end{aligned}$$

■

Formula for quadratic exponential integrals with a linear factor:

$$\int_{-\infty}^{+\infty} xe^{-ax^2+bx+c}\,dx = \left(\frac{b}{2a}\right)\sqrt{\frac{\pi}{a}}\;\exp\left[\frac{b^2}{4a}+c\right]$$

Proof.

$$\begin{aligned}
\int_{-\infty}^{+\infty} xe^{-ax^2+bx+c}\,dx &= \underbrace{\exp\left[\frac{b^2}{4a}+c\right]}_{g}\int_{-\infty}^{+\infty} x\exp\Big[-a\Big(x-\underbrace{\frac{b}{2a}}_{m}\Big)^2\Big]dx \\
&= g\int_{-\infty}^{+\infty} x\exp[-a(x-m)^2]dx \\
&= g\int_{-\infty}^{+\infty} (u+m)e^{-au^2}du \\
&= g\underbrace{\int_{-\infty}^{+\infty} ue^{-au^2}du}_{0} + g\int_{-\infty}^{+\infty} me^{-au^2}du \\
&= g\;m\;\sqrt{\frac{\pi}{a}} \\
&= \left(\frac{b}{2a}\right)\sqrt{\frac{\pi}{a}}\exp\left[\frac{b^2}{4a}+c\right]
\end{aligned}$$

■

Formula for quadratic exponential integrals with a quadratic factor:

$$\int_{-\infty}^{+\infty} x^2 e^{-ax^2+bx+c}\, dx = \left(\frac{b^2+2a}{4a^2}\right)\sqrt{\frac{\pi}{a}}\ \exp\left[\frac{b^2}{4a}+c\right]$$

Proof.

$$\begin{aligned}\int_{-\infty}^{+\infty} x^2 e^{-ax^2+bx+c}\, dx &= g\int_{-\infty}^{+\infty}(u+m)^2 e^{-au^2}du \\ &= g\int_{-\infty}^{+\infty} u^2 e^{-au^2}du + 2mg\underbrace{\int_{-\infty}^{+\infty} ue^{-au^2}du}_{0} + m^2 g\underbrace{\int_{-\infty}^{+\infty} e^{-au^2}du}_{\sqrt{\frac{\pi}{a}}}\end{aligned}$$

Using integration by parts,

$$\begin{aligned}\int_{-\infty}^{+\infty} u^2 e^{-au^2}du &= \int_{-\infty}^{+\infty} u\cdot ue^{-au^2}du \\ &= \underbrace{\left(-\frac{u}{2a}e^{-au^2}\right)\Big|_{u\to-\infty}^{u\to+\infty}}_{0} + \frac{1}{2a}\int_{-\infty}^{+\infty} e^{-au^2}du \\ &= \frac{1}{2a}\sqrt{\frac{\pi}{a}}\end{aligned}$$

And therefore,

$$\begin{aligned}\int_{-\infty}^{+\infty} x^2 e^{-ax^2+bx+c}\, dx &= \frac{g}{2a}\sqrt{\frac{\pi}{a}} + m^2 g\sqrt{\frac{\pi}{a}} \\ &= g\sqrt{\frac{\pi}{a}}\left(\frac{1}{2a}+m^2\right) \\ &= \left(\frac{b^2+2a}{4a^2}\right)\sqrt{\frac{\pi}{a}}\ \exp\left[\frac{b^2}{4a}+c\right]\end{aligned}$$

■

References

[1] Stefano De Leo and Pietro Rotelli. Laser interaction with a dielectric block. *The European Physical Journal D*, 61(2):481–488, 2011.

[2] Max Born and Emil Wolf. *Principles of optics: electromagnetic theory of propagation, interference and diffraction of light*. Elsevier, 2013.

[3] Silvânia A Carvalho and Stefano De Leo. The use of the stationary phase method as a mathematical tool to determine the path of optical beams. *American Journal of Physics*, 83(3):249–255, 2015.

[4] Manoel P Araújo, Stefano De Leo, and Gabriel G Maia. Closed-form expression for the Goos-Hänchen lateral displacement. *Physical Review A*, 93(2):023801, 2016.